ACS Sustainable Chemistry & Engineering

Research Article

pubs.acs.org/journal/ascecg

Highly Photoluminescent Carbon Dots Derived from Egg White: Facile and Green Synthesis, Photoluminescence Properties, and Multiple Applications

Zehui Zhang,‡ Wenhui Sun,‡ and Peiyi Wu*

State Key Laboratory of Molecular Engineering of Polymers, Collaborative Innovation Center of Polymers and Polymer Composite Materials, Department of Macromolecular Science and Laboratory for Advanced Materials, Fudan University, Shanghai 200433, China

Supporting Information

ABSTRACT: Carbon dots, which are superior fluorescent nanomaterials with low photobleaching, low toxicity, excellent biocompatibility, and low environmental hazard, have presented exciting opportunities in many fields. However, a better strategy to synthesize fluorescent carbon dots with high quantum yield and further developing their potential applications is still needed. Herein, a one-step hydrothermal strategy was proposed to prepare carbon dots from egg white. The as-prepared CDs, with a diameter of 2.1 nm, were well-dispersed in aqueous solution and showed excellent pH stability. During the hydrothermal reaction, the carbonization, N-doping, and surface functionalization were realized at the same time. With a high quantum yield of 61%, the CDs were used as a probe for detecting metal ions and in living cell imaging. Additionally, multifunctional nanocomposites were also prepared with novel thermosensitive photoluminescent properties.

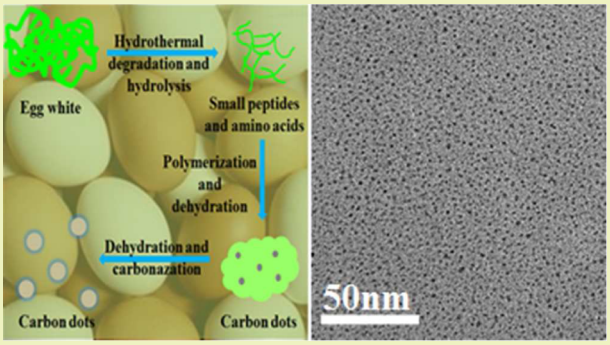

KEYWORDS: *Hydrothermal carbonization, Nitrogen-doped fluorescent carbon nanoparticles, Ions detecting, Cell imaging, Multi-stimuli-responsive nanocomposites*

INTRODUCTION

Carbon nanomaterials (including carbon nanotubes,[1−3] fullerenes,[4,5] nanofibers,[6,7] graphene,[8−10] and other carbonaceous nanomaterials[11,12]) have drawn increasing attention due to their unique properties, such as chemical reactivity, electrical conductivity, and adsorption properties, and show great application prospects in electronic, optical, catalytic, and biological fields.[13−16] Recently, fluorescent carbon dots (CDs), a new class of 0-dimensional carbon nanomaterials, have presented exciting opportunities in bioimaging, disease detection, and drug delivery.[17−23] Compared to organic dyes and traditional semiconductor quantum dots, CDs are superior fluorescent nanomaterials with low photobleaching, low toxicity, excellent biocompatibility, and low environmental hazard. And CDs are thought to be a candidate to replace the traditional semiconducting quantum dots, especially in biology spheres.[24]

A variety of approaches have been developed to prepare photoluminescent (PL) CDs, including laser ablation of graphite,[25,26] vigorous chemical oxidation of carbon sources,[27,28] microwave synthesis,[29,30] and the wet chemical method.[20] Among them, hydrothermal treatment of multiple organic acid/alcohol/amine, amino acid, and protein offers new kinds of facile methods for the fabrication of fluorescent CDs as well as expanding their applications.[31−35] CDs with tunable degree of carbonization generally consist of carbon, hydrogen, and oxygen decorated with numerous functional groups on their surface.[17] Heteroatoms doped (such as S and N) into CDs could improve the fluorescence quantum yield and expand their applications in oxygen reduction reaction and catalysis.[20,31,36,37] Nowadays, using biomass to prepare carbon nanomaterials has been a trend to synthesize heteroatoms doped material because biomass contains abundant heteroatoms.[11,30−32,38−40] However, a better strategy to synthesize fluorescent carbon dots with high quantum yield and further developing their potential applications is still needed.

Eggs are a usual aliment in our daily life with plentiful proteins, carbohydrate, and fat that contain a lot of heteroatoms. Recently, eggs were also used for preparation of CDs.[41,42] Wang and co-workers used rapid plasma treatment of eggs to prepare CDs with a quantum yield of ca. 8%.[41] Qi and co-workers found that microwave treatment of an eggshell membrane can form CDs with a quantum yield of ca. 14%.[42] Herein, we use egg white as a carbon source to prepare CDs

Received: February 27, 2015
Revised: May 22, 2015
Published: June 2, 2015

DOI: 10.1021/acssuschemeng.5b00156
ACS Sustainable Chem. Eng. 2015, 3, 1412−1418

with a simple and green strategy. During the hydrothermal treatment, the carbonization, N-doping, and surface functionalization were realized at the same time, which led to the formation of the CDs with a yield of 31%. The CDs show excellent and stable fluorescent properties with a quantum yield of ca. 61% and were applied as a biosensor reagent for the detection of Fe^{3+}. Additionally, CDs exhibit low toxic and are biocompatible for in living cell imaging and biosensors. Moreover, the CDs were also used to prepare a multifunctional microgel that greatly extends their functions and achieves specific applications in optical devices and light-emitting nanocomposites.

EXPERIMENTAL SECTION

Chemicals. Na_2CO_3, $AgNO_3$, $Al_2(SO4)_3{\cdot}18H_2O$, $CaCl_2$, $CoCl_2{\cdot}6H_2O$, $Cr(NO_3)_3{\cdot}9H_2O$, $CuCl_2{\cdot}2H_2O$, $FeCl_2{\cdot}4H_2O$, $FeCl_3{\cdot}6H_2O$, $Hg(NO_3)_2$, KCl, $MgSO_4$, NaCl, $NiCl_2$, $Pb(NO_3)_2$, and $Zn(OAc)_2{\cdot}2H_2O$, coomassie brilliant blue, and ethanol were purchased from Sinopharm Chemical Reagent Co., Ltd. (China). *N*-isopropylacrylamide (NIPAM) was purchased from Tokyo Kasei Kogyo Co. (Tokyo, Japan). Potassium persulfate (KPS), 1-vinylimidazole (VIM), and *N*,*N*-methylene-bis(acrylamide) (MBAA) (cross-linker) were all purchased from Aladdin reagent Co. Dulbecco's modified Eagle's medium (DMEM, high glucose), 4-(2-hydroxyethyl)-1-piperazineethanesulfonic acid (HEPES), fetal bovine serum, penicillin G, streptomycin, and trypsinase were obtained from GIBCOBRL (Grand Island, New York, USA). 3-(4,5-Dimethylthiazol-2-yl)-2,5-diphenyltetrazolium bromide (MTT) was purchased from Sigma Chemical Co. (St. Louis, MO, USA). All chemicals from commercial sources were used as received without further purification. All aqueous solutions were prepared with Milli-Q water (18.2 MΩ cm^{-1}).

Synthesis of CDs. Fresh chicken eggs were purchased from markets. The egg white was well separated by gauze prior to use. Then the separated egg white was put into a 30 mL Teflon-lined autoclave. Afterward, the autoclave was heated at 220 °C for 48 h and gradually cooled down to room temperature. A yellow CDs suspension was obtained with oily black matter on the autoclave wall. The suspension was filtered to remove the salt precipitate and the oily black matter. Egg yolk was also treated by the same procedure.

Cell Culture and MTT Assay. The cell viability was evaluated on Hela and KB cells using a standard MTT assay. Cells were routinely cultured in flasks and incubated at 37 °C in a humidified hood filled with 5% CO_2. When cells reached 80−90% confluence, they were lifted with trypsin−EDTA. The trypsinized cells were dispersed and diluted in DMEM (high glucose) medium, followed by centrifugation for 5 min at 1000 rpm. After supernatant was removed, the cells were resuspended in DMEM (high glucose) medium and cells number was counted using a hemocytometer. Cells were then plated at a density of approximately 2×10^4 cells per well in a 96-well plate. MTT solution (20 μL, 5 mg mL^{-1}) was added to each well and the cells were incubated for another 4 h. After incubation, the medium was aspirated out and 150 μL of DMSO was added into each well. Absorbance was measured at 570 nm for the calculation of the cell survival rate. The cells cultured with the pure culture medium were set as controls. Three independent experiments were performed under identical conditions.

Living Cell Experiments. Cells were cultured in Dulbecco's modified Eagle's medium (DMEM) supplemented with 10% fetal bovine serum, 100 units mL^{-1} penicillin and 100 μg mL^{-1} streptomycin. For in living cell imaging studies, cells were incubated in DMEM containing 0.04 mg mL^{-1} CDs for 30 min at 37 °C, and washed with phosphate buffer solution (PBS, pH = 7.4) to remove the extracellular remaining CDs for three times. Cells were imaged on a confocal microscope, the excitation wavelength was 400 nm.

Synthesis of P(NIPAM-*co*-VIM)-CDs Microgels. The microgels were prepared using the emulsion polymerization method. Briefly, 0.25 g of NIPAM, 0.013 g of VIM, 0.01 g of BIS, and 0.01 g of SDS were dissolved in 35 mL of water in a three-necked round-bottomed flask. Then add 2 mL of CDs suspension (7.5 mg mL^{-1}) into the flask. The flask purged with nitrogen for 1 h. To initiate the polymerization, 0.008 g of KPS, which was dissolved in water, was added to the mixture at 70 °C. After 15 min, the solution had turned milky white. The reaction proceeded for 4 h under a nitrogen atmosphere and constant stirring. Then the mixture was dialyzed to erase the residual monomer.

Characterization. The transmission electron microscopy (TEM) images were taken with a JEOL JEM-2100 F microscope (Japan) operated at 200 kV equipped with selective area electron diffraction (SAED). Fourier transform infrared (FTIR) spectra were recorded on a Nicolet Nexus 470 spectrometer. UV−vis spectra were measured on a Hitachi U-2910 spectrophotometer. The protein and the intermediate product were detected by an AKTA purifier (GE Healthcare). The sodium dodecyl sulfate-polyacrylamide gel electrophoresis (SDS-PAGE) was performed using 15% precast polyacrylamide gels and Mini-Protean Tetra cell (Tanon, China). X-ray photoelectron spectroscopy (XPS) measurements were taken on a RBD upgraded PHI-5000C ESCA system (PerkinElmer) with Mg Kα radiation ($h\nu$ = 1253.6 eV). Fluorescence spectroscopy was carried out with a Shimadz RF-5301PC spectrophotometer. The absolute quantum yield and the lifetime of the FCNs was determined by an Edinburgh FLS920 spectrophotometer. The temperature-dependent average hydrodynamic radius (Rh) and ζ-potential measurements were performed on a DLS-zetasizer nanosystem (Malvern). The Atomic force microscopy (AFM) measurement was carried out using a Multimode Nano 4 in the tapping mode. The microgels were deposited on a freshly cleaved mica surface.

RESULTS AND DISCUSSION

Physicochemical Characterization. The hydrothermal treatment of egg white at 220 °C leads to a yellow CDs suspension and oily black matter on the top. Figure 1 shows the

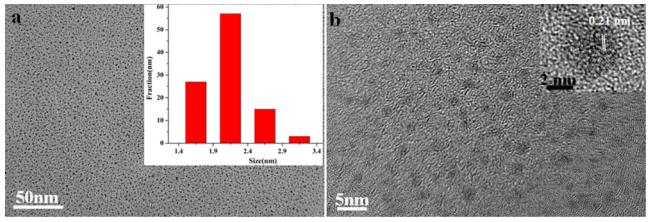

Figure 1. (a) Low magnification TEM images of the CDs thus formed; inset shows the corresponding size distribution of the CDs. (b) High magnification TEM images of the CDs thus formed; inset shows the HRTEM image of the CDs.

TEM image of the as-prepared CD suspension. It is found that their diameters are mainly distributed in the range of 1.4−3.4 nm (Figure 1a, inset). The CDs are uniform in size (an average of ca. 2.1 nm) and well dispersed. The high magnification TEM image in Figure 1b clearly reveals that most particles possess well-resolved lattice fringes. The high-resolution TEM (HRTEM) image (Figure 1b inset) shows parallel graphitic lines with spacing of 0.21 nm, which agrees with that of in-plane lattice spacing of graphene (100 facet). And the upper oily black matter also shows CDs decorated on the big organic matrix with a lot of well crystallized inorganic salt (see Figure S1 of the Supporting Information). As a control, the egg yolk formed carbon nanoparticles with different sizes under same hydrothermal treatment (see Figure S2 of the Supporting Information).

The surface composition and element analysis of the resultant CDs were characterized by XPS. The spectrum shows three distinct peaks at 285.3, 399.4, and 532.0 eV, assigning to C 1s, N 1s, and O 1s peak of CDs, respectively

DOI: 10.1021/acssuschemeng.5b00156
ACS Sustainable Chem. Eng. 2015, 3, 1412−1418

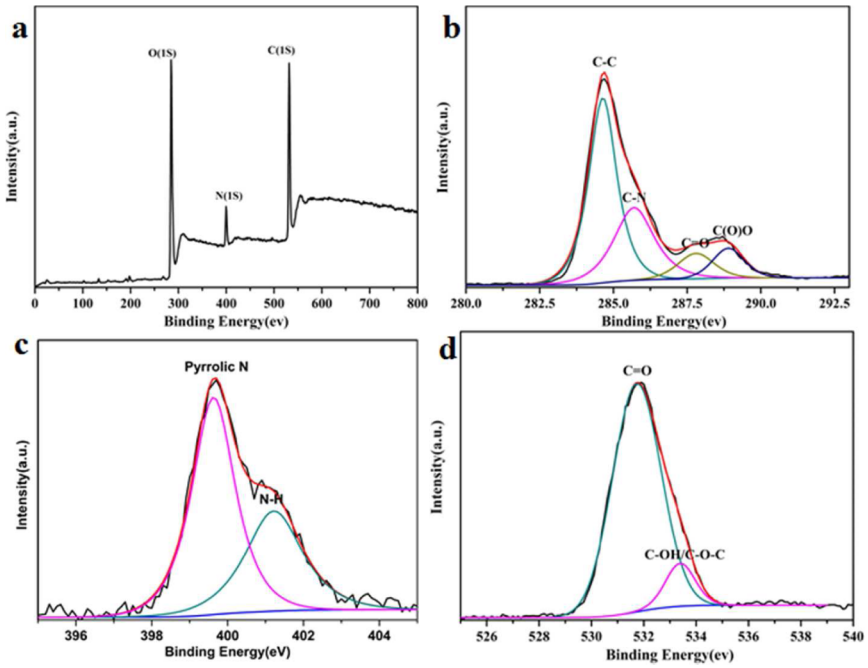

Figure 2. XPS spectra of the CDs thus formed. (a) Survey spectrum. (b) C 1s spectrum. (c) N 1s spectrum. (d) O 1s spectrum.

(Figure 2a). The high-resolution spectrum of C 1s can be assigned to four surface components in the CDs, corresponding to C—C at binding energy of 284.8 eV, C—O and C—N at 286.2 eV, as well as C═O and C═N at 288.4 eV (Figure 2b). In N 1s spectrum, the peaks at 399.6 and 401.2 eV are attributed to pyrrolic-like N and N—H, respectively (Figure 2c). The O 1s spectrum also can be fitted into two peaks at 531.8 and 533.4 eV, assigning to C═O and C—O, respectively (Figure 2d). The elemental analysis results (see Table S1 of the Supporting Information) reveal that the CDs are composed of C (46.40%), H (9.15%), N (13.94%), S (0.12%), and O (calculated, 30.39%) atoms, which is consistent with the XPS results. The chemical and structural information was also confirmed by the FTIR spectrum as shown in Figure S3 of the Supporting Information. The peaks at around 3390 and 3150 cm^{-1} correspond to the O—H and ═C−H stretching mode, respectively. The band at 1670 cm^{-1} can be attributed to the C═C stretching mode of the aromatic hydrocarbons and the C═O stretching mode of the oxygenic groups, and the band at 1400 cm^{-1} is assigned to the bending vibration of C—N deformation. Obviously, it reveals that these CDs derived from the carbonization of egg white are carbon-rich, nitrogen-doped nanodots with a high oxygen content, which are mainly composed of polycyclic aromatic species, as well as hydroxyl, amino and carbonyl/carboxylate groups decorated. The ζ-potential of the CDs was measured to be −17.3 mV, which can also be attributed to hydroxyl and carbonyl groups on the surface.

On the basis of the above analysis, a possible mechanism for the formation of CDs from egg white was proposed (Figure 3). First, the protein in the egg white was hydrolyzed to small low-molecular weight peptide and amino acid at the very beginning of the hydrothermal treatment. This process can be confirmed by the HPLC and the gel electrophoresis results. (see Figures S4 and S5 of the Supporting Information) With the hydrothermal treatment continuing, the amino acids are partially polymerized and then carbonized into CD cores with a lot of oligomers coated (see Figure S6 of the Supporting Information).[11,43] The oligomer coated CD cores grow bigger and the outer oligomers decrease and disappear (see Figure S7 of the Supporting Information). Then we finally got N-doped CDs functionalized with abundant hydroxyl and carboxyl groups. These functionalized groups make the CDs readily dispersed in water and easily functionalized.

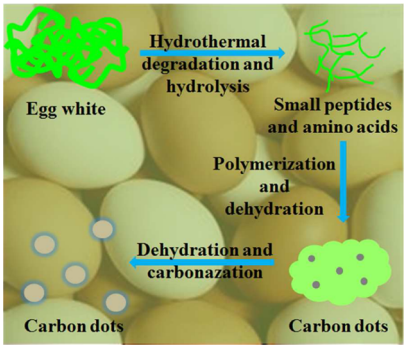

Figure 3. Schematic illustration of the formation mechanism of the CDs.

Photoluminescence Study. The optical properties of CDs were also studied. As shown in Figure 4a, the CDs suspension is light yellow and transparent. And when it was excited under UV light (365 nm), it exhibits strong blue emission. The UV−vis spectrum shows a broad band around the range of 260−290 nm (Figure 4a), which can be seen as a typical absorption of an aromatic system. This peak was also thought to be a characteristic band of fluorescent CDs.[11,20,25,32] The well-dispersed aqueous suspension of CDs exhibits bright blue emission under UV light (365 nm). When these CDs were excited at 315 nm, a maximum emission peak centered at 420 nm was observed. The lifetime of the CDs is 9.1 ns and the absolute quantum yield was 61% (43% by quinine sulfate as a reference). The high quantum yield may be attributed to the abundant surface defects on the N-doped carbon core and the functional groups decorated. There is no bleaching observed

DOI: 10.1021/acssuschemeng.5b00156
ACS Sustainable Chem. Eng. 2015, 3, 1412−1418

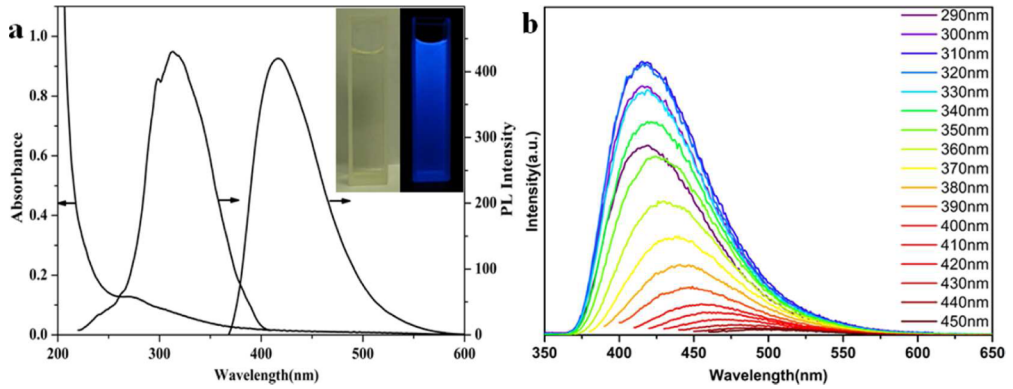

Figure 4. (a) UV−vis absorption and PL spectrum of the CDs in aqueous solution; inset shows the digital photographs of CDs under visible and UV light (365 nm). (b) Emission spectra of the CDs recorded with progressively longer excitation wavelength in 10 nm increments.

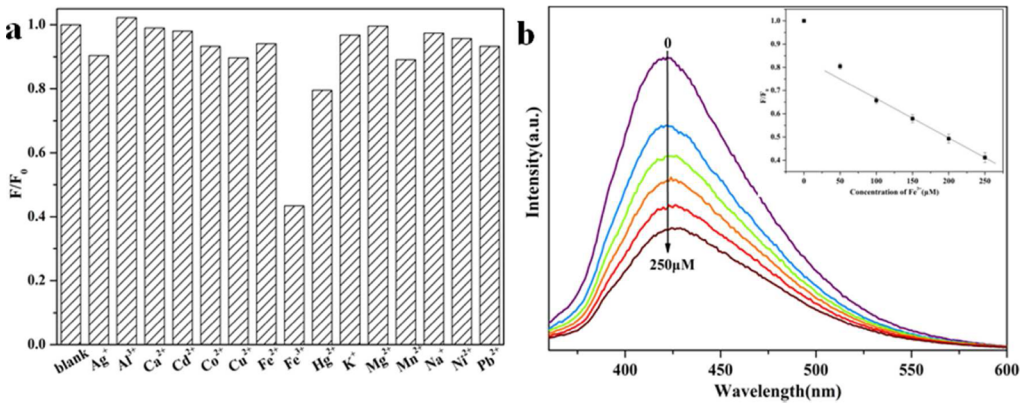

Figure 5. (a) Comparison of fluorescence intensities of CDs after the addition of different metal ions. (b) Fluorescence quenching in the presence of Fe^{3+} ions; inset shows the plot of F/F_0 (F_0 and F are the highest fluorescence intensities of CDs excited at 315 nm in the absence and presence of Fe^{3+}) as a function of the Fe^{3+} concentrations ions within the range of 0−250 μM.

after irradiation with UV light, and the photoluminescence of the CDs did not change a lot under the UV irradiation for 12 h, which suggests that the CDs photoluminescence was very stable (see Figure S8 of the Supporting Information). The CDs also show similar excitation-dependent PL behavior as the previously reported fluorescent carbon nanodots: with the excitation wavelength changing from 290 to 450 nm, the strongest emission peak shifts from 415 to 540 nm and the intensity decreases rapidly (Figure 4b).[20,32,39] This interesting excitation-dependent PL behavior might be used in multicolor imaging applications. The qualitative relationship between pH value and emission was further studied (Figure S9 of the Supporting Information). The CDs possess excellent pH stability, preserving stable fluorescence at pH values between 3 and 12, which made them a good probe for detecting ions without affecting by pH in different environment conditions. However, the fluorescence of the CDs was easily affected by the solvents (see Figure S10 of the Supporting Information). That may be attributed to the poor dispersibility of the CDs in these solvents.

Ions Detecting. It should be mentioned that the aqueous suspension of the CDs is very stable. The fluorescence intensity is almost unabated after more than 6 months, which offers more advantages for its future applications. The selectivity of the sensing system by CDs was evaluated: many different metal ions, such as Ag^+, Al^{3+}, Ca^{2+}, Cd^{2+}, Co^{3+}, Cu^{2+}, Fe^{2+}, Fe^{3+}, Hg^{2+}, K^+, Mg^{2+}, Mn^{2+}, Na^+, Ni^{2+}, and Pb^{2+}, were detected under the same conditions (Figure 5a). It shows that Fe^{3+} has the greatest fluorescence quenching effect among these metal ions, which means the CDs are more sensitive and reliable for the detection of Fe^{3+} ion than other metal ions. The fluorescence intensity gradually decreases with increasing the concentration of Fe^{3+} ions and the I/I_0 shows good linearity with the Fe^{3+} concentration in the range of around 50 to 250 μM, as shown in Figure 5b. The linear range meets the requirement in sensing of Fe^{3+} ion, thus the samples can be used as a fluorescent probe for real-time tracking of Fe^{3+} ion. The slight quenching of other ions, such as Ag^+, Co^{2+}, Cu^{2+}, Fe^{2+}, Hg^{2+}, and Ni^{2+}, can be attributed to the nonspecific electrostatic interactions between carboxylic groups and metal ions.

Cell Imaging. The possible application of CDs as cell-imaging agents was also explored. The inherent cytotoxicity of CDs was evaluated using Hela and KB living cells lines through MTT (MTT = 3-(4,5-dimethylthiazol-2-yl)-2,5-diphenyltetrazolium bromide) assay. The cell viabilities of Hela and KB cells were tested after being exposed to CDs at different concentrations (see Figure S12 of the Supporting Information). As observed, the cell survival rate of both cells upon addition of the CDs was between 80 and 100% at up to 80 mg mL^{-1} and long incubation time (24 h), which suggests that the CDs have low cytotoxicity and are safe for in vitro applications. Thus, the CDs can be a suitable probe for cell imaging: CD solution has been mixed with cell culture media along with Hela cells, incubated for 30 min, and the cells were washed three times to remove the extracellular remaining CDs. The washed cells were then imaged under blue, bright field, and overlapped excitations

DOI: 10.1021/acssuschemeng.5b00156
ACS Sustainable Chem. Eng. 2015, 3, 1412−1418

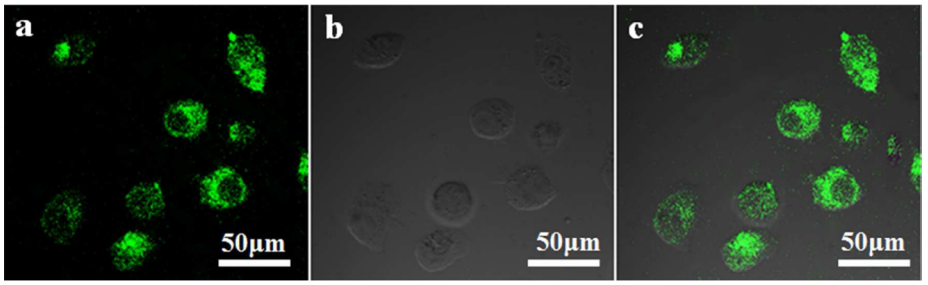

Figure 6. Confocal laser scanning microscopy images of living Hela cells incubated for 30 min at 37 °C in DMEM containing 0.04 mg mL^{-1} of the CDs: (a) collected from the emission wavelength channel: 475−525 nm (λex = 400 nm). (b) Corresponding bright-field images and (c) overlapped images of the living cells.

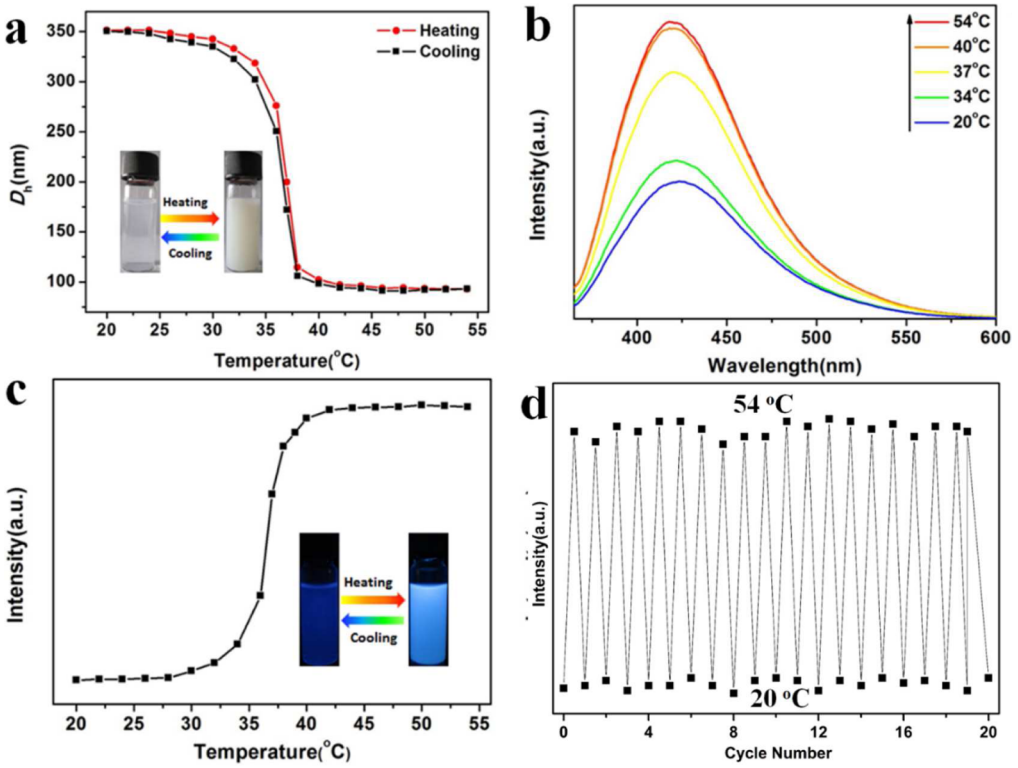

Figure 7. (a) DLS (1.0 mg mL^{-1}) measurements of P(NIPAM-*co*-VIM)-CDs in H_2O during heating with increments of 2 °C from 20 to 54 °C; inset shows the digital photographs of CDs under daylight at different temperatures. (b) Emission spectra of the P(NIPAM-*co*-VIM)-CDs microgels at different temperatures. (c) PL intensity of the P(NIPAM-*co*-VIM)-CDs microgels at different temperatures, inset shows the digital photographs of CDs under UV light (365 nm) at different temperatures. (d) PL intensity of the P(NIPAM-*co*-VIM)-CDs microgels as a function of heating−cooling cycles between 20 and 54 °C.

(Figure 6a,b,c). The blue excitation images of Hela cells clearly show the green fluorescent CDs inside the cells (Figure6a). The bright-field and overlapped fluorescence images (Figure 6b,c) reveal that the fluorescence signals are from the cytosol leaving zones of nuclei. These results clearly indicate good cell-permeability of the CDs into living cells. So, the CDs can be seen as a probe biocompatible for living cell imaging and biosensors.

P(NIPAM-*co*-VIM)-CDs Microgels. To investigate further the capability of CDs, multi-stimuli-responsive microgels were prepared by the emulsion polymerization technique through the copolymerization of 1-vinylimidazole (VIM) and *N*-isopropylacrylamide (NIPAM) at 70 °C with methylene-bis-acrylamide (MBAA) as a cross-linker. The imidazole ring can easily be protonated and has a positive charge that can be effectively absorbed on the CDs via the electrostatic force. Then the CDs in the microgel can be an effective physical cross-linking point. TEM and SEM images show that the microgels are uniform with average size of ∼200 nm (see Figure S12a,b of the Supporting Information). The structures of the microgels were further characterized by atom force microscopy (AFM, see Figure S13 of the Supporting Information). The images suggest that the microgels are monodispersed, with a size of ca. 200 nm in diameter, but only ca. 6 nm in height. This height distortion may be attributed to the structure collapse of the microgels during the preparation process for AFM testing samples. The temperature sensitivity of the microgels was also studied: the microgel showed obvious phase transformation with the increase of the temperature (Figure 7a). Because of the good dispersion and strong fluorescence of the CDs in the microgel, the PL properties of the obtained P(NIPAM-*co*-VIM)-CDs microgels show similar

DOI: 10.1021/acssuschemeng.5b00156
ACS Sustainable Chem. Eng. 2015, 3, 1412−1418

temperature sensitivity (Figure 7b,c). At low temperatures, the P(NIPAM-*co*-VIM)-CDs microgels are transparent and show similar fluorescence as the CDs under UV light. With the increase of the temperature, the PL intensity of the P(NIPAM-*co*-VIM)-CDs microgels increases slowly and a sharp increase can be found at around 36 °C, which is the same as the DLS results. Moreover, the microgels shows good reversibility after 20 cycles of heating−cooling process, indicating its bright future to prepare thermosensitive sensors (Figure 7d, and Figure S14 of the Supporting Information). Different from the previously reported hydrogel,[44−46] the unique temperature sensitivity of the microgels might be attributed to the charge density change of the microgels during the phase transition process, which can effectively affect the electrostatic interaction between the polymer chains and the CDs.[47,48] As shown in Figure S15 of the Supporting Information, an increase in ζ-potential of the microgels in water is observed with the temperature increasing from 32 to 42 °C. The positive value of ζ-potential is reasonable in neutral solutions; because the imidazole group is a weak base, polyvinyl imidazole becomes protonated. Then we can conclude that as shown in Figure S16 of the Supporting Information, at low temperatures, the CDs were entrapped in the microgel network, and most of the CDs were at self-quenching concentration.[49] With increased temperature, the polymer matrix collapsed, the PNIPAM on the exterior of the microgels became hydrophobic and aggregated into the interior of the microgels. The CDs are forced to be outside the PNIPAM composite particles and may have more opportunities to contact water; as a result, the self-quenching effect decreased and fluorescence intensity increased even though the increments in the scattering of the collapsed polymer matrix have the opposite effects.[45,50,51]

CONCLUSIONS

In summary, a facile and high-output method for the fabrication of CDs with a quantum yield as high as ca. 61% was developed by hydrothermal treatment of egg white. During the hydrothermal reaction, the carbonization, N-doping, and surface functionalization were realized at the same time. With no pH sensitivity, the prepared CDs were used as a probe to detect Fe^{3+}. By combining attractive fluorescent properties with good biocompatibility, the obtained CDs were also used as a label for in vitro bioimaging, which demonstrates an immense potential for biomedical application. Moreover, the CDs were also used for fabrication of microgels with thermosensitive PL properties. Thus, CDs synthesis from egg white shows great promise for application in biomedical imaging and biomedicine and opens up enormous opportunities for multifunctional devices or sensors.

ASSOCIATED CONTENT

Supporting Information

TEM images of the upper oily black matter, IR spectra of CDs, element analysis results of the egg white and CDs, TEM images of the CDs with different reaction time, pH effect on the CDs fluorescence intensity, cell viability values, TEM, SEM and AFM images of microgels, schematic illustration of the networks of P(NIPAM-*co*-VIM)-CDs microgels, etc. The Supporting Information is available free of charge on the ACS Publications website at DOI: 10.1021/acssuschemeng.5b00156.

AUTHOR INFORMATION

Corresponding Author

*P. Wu. E-mail: peiyiwu@fudan.edu.cn.

Author Contributions

‡These authors contributed equally.

Notes

The authors declare no competing financial interest.

ACKNOWLEDGMENTS

We gratefully acknowledge the financial support from the National Science Foundation of China (NSFC) (Nos. 21274030, 51473038).

REFERENCES

(1) Baughman, R. H.; Zakhidov, A. A.; de Heer, W. A. Carbon nanotubes - The route toward applications. *Science* **2002**, *297*, 787−792.

(2) Welsher, K.; Liu, Z.; Sherlock, S. P.; Robinson, J. T.; Chen, Z.; Daranciang, D.; Dai, H. A route to brightly fluorescent carbon nanotubes for near-infrared imaging in mice. *Nat. Nanotechnol.* **2009**, *4*, 773−780.

(3) Yang, N.; Chen, X.; Ren, T.; Zhang, P.; Yang, D. Carbon nanotube based biosensors. *Sens. Actuators, B* **2015**, *207*, 690−715.

(4) Jeong, J.; Jung, J.; Choi, M.; Kim, J. W.; Chung, S. J.; Lim, S.; Lee, H.; Chung, B. H. Color-tunable photoluminescent fullerene nanoparticles. *Adv. Mater.* **2012**, *24*, 1999−2003.

(5) Lai, Y.-Y.; Cheng, Y.-J.; Hsu, C.-S. Applications of functional fullerene materials in polymer solar cells. *Energy Environ. Sci.* **2014**, *7*, 1866−1883.

(6) Peng, J.; Gao, W.; Gupta, B. K.; Liu, Z.; Romero-Aburto, R.; Ge, L.; Song, L.; Alemany, L. B.; Zhan, X.; Gao, G.; Vithayathil, S. A.; Kaipparettu, B. A.; Marti, A. A.; Hayashi, T.; Zhu, J.-J.; Ajayan, P. M. Graphene quantum dots derived from carbon fibers. *Nano Lett.* **2012**, *12*, 844−849.

(7) Xu, X.; Zhou, J.; Jiang, L.; Lubineau, G.; Payne, S. A.; Gutschmidt, D. Lignin-based carbon fibers: Carbon nanotube decoration and superior thermal stability. *Carbon* **2014**, *80*, 91−102.

(8) Geim, A. K. Graphene: Status and prospects. *Science* **2009**, *324*, 1530−1534.

(9) Han, W.; Ren, L.; Gong, L.; Qi, X.; Liu, Y.; Yang, L.; Wei, X.; Zhong, J. Self-assembled three-dimensional graphene-based aerogel with embedded multifarious functional nanoparticles and its excellent photoelectrochemical activities. *ACS Sustainable Chem. Eng.* **2014**, *2*, 741−748.

(10) Zhu, J.; Yang, D.; Yin, Z.; Yan, Q.; Zhang, H. Graphene and graphene-based materials for energy storage applications. *Small* **2014**, *10*, 3480−3498.

(11) Li, W.; Zhang, Z.; Kong, B.; Feng, S.; Wang, J.; Wang, L.; Yang, J.; Zhang, F.; Wu, P.; Zhao, D. Simple and green synthesis of nitrogen-doped photoluminescent carbonaceous nanospheres for bioimaging. *Angew. Chem., Int. Ed.* **2013**, *52*, 8151−8155.

(12) Huang, Y.; Wang, Y.; Li, Z.; Yang, Z.; Shen, C.; He, C. Effect of pore morphology on the dielectric properties of porous carbons for microwave absorption applications. *J. Phys. Chem. C* **2014**, *118*, 26027−26032.

(13) Stankovich, S.; Dikin, D. A.; Dommett, G. H. B.; Kohlhaas, K. M.; Zimney, E. J.; Stach, E. A.; Piner, R. D.; Nguyen, S. T.; Ruoff, R. S. Graphene-based composite materials. *Nature* **2006**, *442*, 282−286.

(14) Yamashita, T.; Yamashita, K.; Nabeshi, H.; Yoshikawa, T.; Yoshioka, Y.; Tsunoda, S.-i.; Tsutsumi, Y. Carbon nanomaterials: Efficacy and safety for nanomedicine. *Materials* **2012**, *5*, 350−363.

(15) Trogadas, P.; Fuller, T. F.; Strasser, P. Carbon as catalyst and support for electrochemical energy conversion. *Carbon* **2014**, *75*, 5−42.

(16) Xu, M.; He, G.; Li, Z.; et al. A green heterogeneous synthesis of N-doped carbon dots and their photoluminescence applications in solid and aqueous states. *Nanoscale* **2014**, *6*, 10307−10315.

(17) Baker, S. N.; Baker, G. A. Luminescent carbon nanodots: Emergent nanolights. *Angew. Chem., Int. Ed.* **2010**, *49*, 6726−6744.
(18) Ray, S. C.; Saha, A.; Jana, N. R.; Sarkar, R. Fluorescent carbon nanoparticles: Synthesis, characterization, and bioimaging application. *J. Phys. Chem. C* **2009**, *113*, 18546−18551.
(19) Zhu, A.; Qu, Q.; Shao, X.; Kong, B.; Tian, Y. Carbon-dot-based dual-emission nanohybrid produces a ratiometric fluorescent sensor for in vivo imaging of cellular copper ions. *Angew. Chem.* **2012**, *124*, 7297−7301.
(20) Xu, Y.; Wu, M.; Liu, Y.; Feng, X.-Z.; Yin, X.-B.; He, X.-W.; Zhang, Y.-K. Nitrogen-doped carbon dots: A facile and general preparation method, photoluminescence investigation, and imaging applications. *Chem.—Eur. J.* **2013**, *19*, 2276−2283.
(21) Luo, P. G.; Yang, F.; Yang, S.-T.; Sonkar, S. K.; Yang, L.; Broglie, J. J.; Liu, Y.; Sun, Y.-P. Carbon-based quantum dots for fluorescence imaging of cells and tissues. *Rsc Adv.* **2014**, *4*, 10791−10807.
(22) Lim, S. Y.; Shen, W.; Gao, Z. Carbon quantum dots and their applications. *Chem. Soc. Rev.* **2015**, *44*, 362−381.
(23) Li, H.; Chen, L.; Wu, H.; He, H.; Jin, Y. Ionic liquid-functionalized fluorescent carbon nanodots and their applications in electrocatalysis, biosensing, and cell imaging. *Langmuir* **2014**, *30*, 15016−15021.
(24) Wang, L.; Yin, Y.; Jain, A.; Zhou, H. S. Aqueous phase synthesis of highly luminescent, nitrogen-doped carbon dots and their application as bioimaging agents. *Langmuir* **2014**, *30*, 14270−14275.
(25) Cao, L.; Wang, X.; Meziani, M. J.; Lu, F.; Wang, H.; Luo, P. G.; Lin, Y.; Harruff, B. A.; Veca, L. M.; Murray, D.; Xie, S.-Y.; Sun, Y.-P. Carbon dots for multiphoton bioimaging. *J. Am. Chem. Soc.* **2007**, *129*, 11318−11319.
(26) Qin, Y.; Cheng, Y.; Jiang, L.; Jin, X.; Li, M.; Luo, X.; Liao, G.; Wei, T.; Li, Q. Top-down strategy toward versatile graphene quantum dots for organic/inorganic hybrid solar cells. *ACS Sustainable Chem. Eng.* **2015**, *3*, 637−644.
(27) Zheng, L.; Chi, Y.; Dong, Y.; Lin, J.; Wang, B. Electrochemiluminescence of water-soluble carbon nanocrystals released electrochemically from graphite. *J. Am. Chem. Soc.* **2009**, *131*, 4564−4565.
(28) Hu, C.; Yu, C.; Li, M.; Wang, X.; Yang, J.; Zhao, Z.; Eychmueller, A.; Sun, Y. P.; Qiu, J. Chemically tailoring coal to fluorescent carbon dots with tuned size and their capacity for Cu(II) detection. *Small* **2014**, *10*, 4926−4933.
(29) Zhu, H.; Wang, X.; Li, Y.; Wang, Z.; Yang, F.; Yang, X. Microwave synthesis of fluorescent carbon nanoparticles with electrochemiluminescence properties. *Chem. Commun.* **2009**, 5118−5120.
(30) Gong, N.; Wang, H.; Li, S.; Deng, Y.; Chen, X. a.; Ye, L.; Gu, W. Microwave-assisted polyol synthesis of gadolinium-doped green luminescent carbon dots as a bimodal nanoprobe. *Langmuir* **2014**, *30*, 10933−10939.
(31) Zhu, C.; Zhai, J.; Dong, S. Bifunctional fluorescent carbon nanodots: Green synthesis via soy milk and application as metal-free electrocatalysts for oxygen reduction. *Chem. Commun.* **2012**, *48*, 9367−9369.
(32) Kozák, O.; Datta, K. K. R.; Greplová, M.; Ranc, V.; Kašlík, J.; Zbořil, R. Surfactant-derived amphiphilic carbon dots with tunable photoluminescence. *J. Phys. Chem. C* **2013**, *117*, 24991−24996.
(33) Park, S. Y.; Lee, H. U.; Park, E. S.; Lee, S. C.; Lee, J.-W.; Jeong, S. W.; Kim, C. H.; Lee, Y.-C.; Huh, Y. S.; Lee, J. Photoluminescent green carbon nanodots from food-waste-derived sources: Large-scale synthesis, properties, and biomedical applications. *ACS Appl. Mater. Interfaces* **2014**, *6*, 3365−3370.
(34) Li, Q.; Ohulchanskyy, T. Y.; Liu, R.; Koynov, K.; Wu, D.; Best, A.; Kumar, R.; Bonoiu, A.; Prasad, P. N. Photoluminescent carbon dots as biocompatible nanoprobes for targeting cancer cells in vitro. *J. Phys. Chem. C* **2010**, *114*, 12062−12068.
(35) Yang, Z.; Xu, M.; Liu, Y.; He, F.; Gao, F.; Su, Y.; Wei, H.; Zhang, Y. *Nanoscale* **2014**, *6*, 1890−1895.
(36) Huang, H.; Li, C.; Zhu, S.; Wang, H.; Chen, C.; Wang, Z.; Bai, T.; Shi, Z.; Feng, S. Histidine-derived nontoxic nitrogen-doped carbon dots for sensing and bioinnaging applications. *Langmuir* **2014**, *30*, 13542−13548.
(37) Ding, H.; Wei, J.-S.; Xiang, H.-M. Nitrogen and sulfur co-doped carbon dots with strong blue luminescence. *Nanoscale* **2014**, *6*, 13817−13823.
(38) Liu, S.; Tian, J.; Wang, L.; Zhang, Y.; Qin, X.; Luo, Y.; Asiri, A. M.; Al-Youbi, A. O.; Sun, X. Hydrothermal treatment of grass: A low-cost, green route to nitrogen-doped, carbon-rich, photoluminescent polymer nanodots as an effective fluorescent sensing platform for label-free detection of Cu(II) ions. *Adv. Mater.* **2012**, *24*, 2037−2041.
(39) Ruan, S.; Qian, J.; Shen, S.; Zhu, J.; Jiang, X.; He, Q.; Gao, H. A simple one-step method to prepare fluorescent carbon dots and their potential application in non-invasive glioma imaging. *Nanoscale* **2014**, *6*, 10040−10047.
(40) Liu, S.-S.; Wang, C.-F.; Li, C.-X.; Wang, J.; Mao, L.-H.; Chen, S. Hair-derived carbon dots toward versatile multidimensional fluorescent materials. *J. Phys. Chem. C* **2014**, *2*, 6477−6483.
(41) Wang, J.; Wang, C.-F.; Chen, S. Amphiphilic egg-derived carbon dots: rapid plasma fabrication, pyrolysis process, and multicolor printing patterns. *Angew. Chem., Int. Ed.* **2012**, *51*, 9297−9301.
(42) Wang, Q.; Liu, X.; Zhang, L.; Lv, Y. Microwave-assisted synthesis of carbon nanodots through an eggshell membrane and their fluorescent application. *Analyst* **2012**, *137*, 5392−5397.
(43) Shang, S.; Wang, H. Study on microwave hydrolysis for the analysis of amino acids in egg by high performance liquid chromatography. *Chin. J. Chromatogr.* **1997**, *15*, 138−140.
(44) Mathkar, A.; Narayanan, T. N.; Alemany, L. B.; Cox, P.; Nguyen, P.; Gao, G.; Chang, P.; Romero-Aburto, R.; Mani, S. A.; Ajayan, P. M. Synthesis of fluorinated graphene oxide and its amphiphobic properties. *Part. Part. Syst. Charact.* **2013**, *30*, 266−272.
(45) Zhou, L.; He, B.; Huang, J. Amphibious fluorescent carbon dots: One-step green synthesis and application for light-emitting polymer nanocomposites. *Chem. Commun.* **2013**, *49*, 8078−8080.
(46) Yin, J.-Y.; Liu, H.-J.; Jiang, S.; Chen, Y.; Yao, Y. Hyperbranched polymer functionalized carbon dots with multistimuli-responsive property. *ACS Macro Lett.* **2013**, *2*, 1033−1037.
(47) Kratz, K.; Hellweg, T.; Eimer, W. Influence of charge density on the swelling of colloidal poly(N-isopropylacrylamide-co-acrylic acid) microgels. *Colloids Surf., A* **2000**, *170*, 137−149.
(48) Dou, H.; Yang, W.; Tao, K.; Li, W.; Sun, K. Thermal sensitive microgels with stable and reversible photoluminescence based on covalently bonded quantum dots. *Langmuir* **2010**, *26*, 5022−5027.
(49) Zhao, X.; Zhu, S.; Song, Y.; Zhang, J.; Yang, B. Thermal responsive fluorescent nanocomposites based on carbon dots. *RSC Adv.* **2015**, *5*, 15187−15193.
(50) Panpan, L.; Lei, H.; Youjie, L.; Leo, S.; Qi, C.; Wangzhou, S. Printable temperature-responsive hybrid hydrogels with photoluminescent carbon nanodots. *Nanotechnology* **2014**, *25*, 055603.
(51) Agrawal, M.; Rubio-Retama, J.; Zafeiropoulos, N. E.; Gaponik, N.; Gupta, S.; Cimrova, V.; Lesnyak, V.; López-Cabarcos, E.; Tzavalas, S.; Rojas-Reyna, R.; Eychmüller, A.; Stamm, M. Switchable Photoluminescence of CdTe Nanocrystals by temperature-responsive microgels. *Langmuir* **2008**, *24*, 9820−9824.

DOI: 10.1021/acssuschemeng.5b00156
ACS Sustainable Chem. Eng. 2015, 3, 1412−1418